

# Solving the Problem of Friction and Wear in Auxiliary Devices of Internal Combustion Engines on the Example of Reciprocating Air Compressor for Vehicles

Saša MILOJEVIĆ\*, Slobodan SAVIĆ, Slobodan MITROVIĆ, Dejan MARIĆ\*, Božidar KRSTIĆ, Blaža STOJANOVIĆ, Vladimir POPOVIĆ

**Abstract:** Using vehicles and other mobile systems to transport passengers and goods, approximately 25% of Europe's greenhouse gases are generated. At the same time, many research papers, published by researchers and students, promote the use of electric vehicles as zero-emission vehicles. Given that, more broadly, the emission of electric vehicles is higher, especially in countries where electricity is obtained by burning coal, the use of internal-combustion engines is still dominant. There are other reasons for using an internal-combustion engine, such as already developed pumping station infrastructure, which is not the case when recharging electric vehicles. Improvements in engine design contribute to meet the regulations relating to the fuel consumption and toxic gas emissions. This refers to the use of alternative fuels, improving the combustion process, and increasing efficiency (efficiency coefficient) by reducing losses. The research is focused on the problem of friction and wear in internal combustion engines and reciprocating air compressors, as auxiliary devices on engines. For that purpose, construction of the reciprocating air compressor in motor vehicles was redesigned. The paper presents the characteristic test results of material used to strengthen liner of the aluminum cylinder. Specifically, a method for testing the performance characteristics of a single-cylinder reciprocating compressor inside of an experimental installation for compressed air supply has also been proposed.

**Keywords:** air compressor; aluminum; friction; internal combustion engine; wear

## 1 INTRODUCTION

It is estimated that about 30% of the total American energy needs and 70% of the American oil consumption are engaged in the transport sector. In addition, the average American household spends more than 15% of total family expenses on transportation, making it the most expensive category of consumption after housing [1]. Similar scenario is also observed in the European Union [2].

New technologies have been developed and applied to vehicles and their propulsion systems for higher fuel economy and lower raw emissions of toxic gasses. This primarily refers to the electrification of vehicles and their propulsion systems [3, 4].

On the other hand, a lot of funds are invested in research work to encourage development in internal combustion (IC) engines [4, 5].

Generally, the use of new lightweight materials or eco-tribology measures (surface change for example) in vehicles and engines is important for lowering the fuel consumption, while the propulsion and mobile systems for keeping projected safety and performance. By applying these technologies only inside the passenger vehicles, one can improve fuel economy by 6-8% for each 10% reduction in weight [1, 6, 7].

Mechanical losses (consisting of friction and parasitic losses in auxiliary units) in IC engines, can be reduced by improving tribology situation of sliding contact between two metal surfaces. That refers to light-weighting of sliding parts, reducing production tolerances to improve the fit between piston and cylinder liner, and improving the lubrication between sliding parts with proposed innovative contacts [8-11].

To improve tribology characteristics the classic production technologies, as honing of cylinder surface, and different surface textures, were used before [12, 13].

If aluminum is used as lightweight material for pistons and cylinders, the problems are lower mechanical hardness and intense wear during sliding contact [14, 15].

The above cited problems are resolved by applying anti-friction coatings and composite materials [16-18].

As contribution, we started the research in domain of IC engines, by optimization of combustion process with introduction of variable compression ratio (VCR) technologies, first in experimental gasoline engine and after that in diesel engine [19, 20].

After that we are continuing with researches and tribology characteristics optimization in domain of reciprocating air compressors made of aluminum alloy. In the manuscript we are presenting some results of performed experimental researches [21-23].

## 2 RESEARCH METRHODS

### 2.1 Material and Methods for Testing the Performance of Reciprocating Compressor

During research, we used the reciprocating compressor for production of compressed air for braking systems inside heavy truck and buses, as well as trains and construction machinery. Concretely, for this purpose, the cylinder was redesigned. Ferrous based cylinder construction was replaced with aluminum alloy AlSi10Mg. Because of the lower hardness of aluminum alloy compared to cast iron, the inner cylinder surface is reinforced with inserts on the cast iron basis.

This problem is first resolved by applying ferrous-based coatings, Fig. 1. In this way, the inner cylinder surface was treated with melted material made of steel by applied spraying technology in atmospheric conditions. Similar experiments are being done in the domain of IC engines, specifically with the cylinders, valve seats, bearings etc. According to available results in the cited literature, different coatings resolve the problems of friction as well as wear. Globally, research shows that the application of coatings contributes to reducing emissions and fuel consumption indirectly, thus contributing to the preservation of the human environment and energy reserves [23-25].

As the second solution, it is proposed to strengthen the sliding surface of the cylinder with reinforcements made of tribological material. The cylinder is reinforced similar in texture to an iron-based material. A reinforcement option

in the form of a graphite or copper texture has also been proposed, Fig. 1 [26].

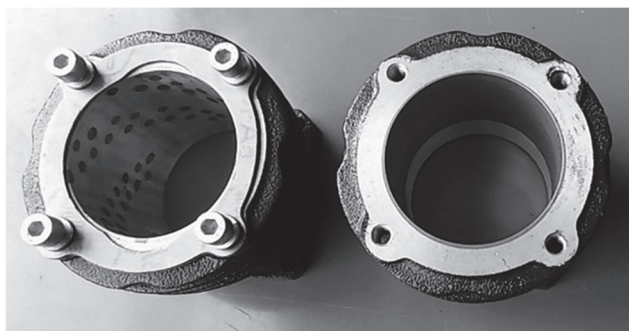


**Figure 1** Cylinders prepared for installation. From left: with reinforcement (circular oval plates) and right: coated by thermal spray method

The goal of reconstruction is to predetermine sliding contact of the piston rings and cylinder liner by putting tribology reinforcements between. In this way, contact with lower friction and wear is achieved. The reconstruction was performed partly according to the guidelines for the application of green tribology measures in engineering [27].

The reason for this reconstruction is the real condition of the cylinder liner after machining in production. The cylinder is of oval shape and porous with grooves, which is why during work it is difficult to do stable contact along the circumference of the piston rings [28, 29].

Due to the oval shape (no circularity) of the cylinder, there is an eccentricity between the axis of the cylinder and the piston in the operation of the machine. As a result, the intensity of the forces between the cylinder liner and the piston rings is variable, causing intense friction and wear [30, 31].

Tribology optimized innovative cylinder for reciprocating compressors, is part of the specifically designed test bench for performance testing of air compressor in real conditions. This means that experimental results are obtained just on tribology experiments with reciprocating motion between the sphere made of steel and a plate made of tested material. For final material selection for the cylinder liner, we needed experimental research in real conditions. Compressor performance testing is performed according to standardized procedure. Specifically, model of compressed air delivery system has been proposed and accepted for this purpose, Fig. 2.

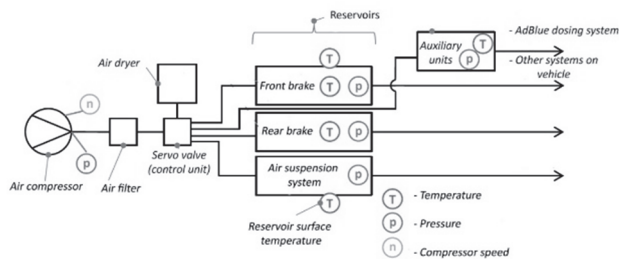


**Figure 2** Model of experimental installation for compressed air supply (Simulation of installation for delivery of compressed air to the systems on the vehicle or other mobile system)

In this way, we can use the standard procedure, on determining the actual performance characteristics of the compressor, concretely power and free air delivery (FAD)

[32]. Based on the obtained results, the optimized cylinder construction can be selected from the aspect of reducing mechanical losses (friction and wear).

Optimization of mechanical losses of the reciprocating compressor is the subject of other planned research. The paper presents only the results of tribology research.

## 2.2 Experimental Data and Conditions

Tribology testing was performed using a tribometer (manufacturer CSM Instruments) under ASTM G133-05 test method in environmental conditions. In the tribometer, a sphere like a counter body on cantilever is loaded onto the sample of material in the form of a plate, Fig. 3. The set conditions correspond most to the real ones inside the cylinder [33, 34].

More detailed testing conditions are shown in the literature [35]. The examination of the material was conducted at three different values of force and speed of reciprocating motion, whose values simulate the real conditions in the cylinder. The results shown were obtained at a low load, both at lower and higher reciprocating speed of testing of the sample material.

Penetration depth was also measured under a performed scratch test on material sample.

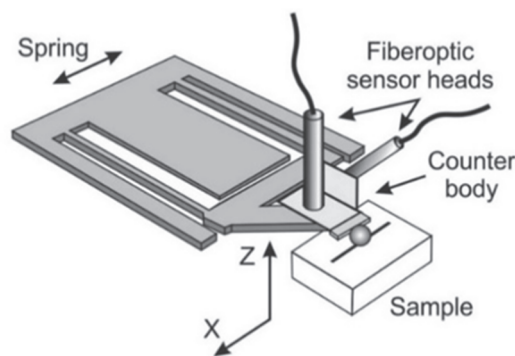


**Figure 3** CSM tribometer module for realization of reciprocating motion between the sphere made of steel and a plate made of tested material

Testing was performed with a total of 500 contact cycles (lap number) on each regime. This corresponded to a reciprocating motion distance of 1 m, and one-half amplitude of 0.5 mm. The acquisition was realized at a frequency of 50 Hz.

The software used for data processing has a commercial name TriboX 2.9.0. For scratch test, the scratches or wear rate as well as volume of wear traces are calculated through penetration depth value for each test regime.

By using an optical microscope, it released the measurement of scratches to determine the wear rate of the tested material. A fully automatized microscope with specifically designed software (SEM-Scanning Electron Microscope; manufacturer Meiji Techno) was used for this purpose.

To obtain a micrograph and chemical composition for detailed analysis of characteristic regions on worn material EDS-Energy-Dispersive Spectroscopy was used. For this purpose, the system was equipped with Phenom ProX Desktop SEM with EDS capability or SEM/EDS system.

The samples prepared for analysis of the microstructure were polished mechanically, and then cleaned with ethanol, Fig. 4.

### 3 RESULTS OF TRIBOLOGY RESEARCH

#### 3.1 SEM/EDS Analysis of the Aluminum Cylinder Liner with Cast Iron Reinforcement

Fig. 4 shows photography and microstructure of a sample prepared for SEM/EDS analysis. In this particular case, the characteristic zone of the sample (transition between base material and reinforcement) was analyzed.

The SEM observation of this sample indicated five characteristic points (zones) on micrograph. The microstructure and EDS analyses of cylinder surface in the

above indicated points are shown in the diagrams below, Fig. 5 to Fig. 9.

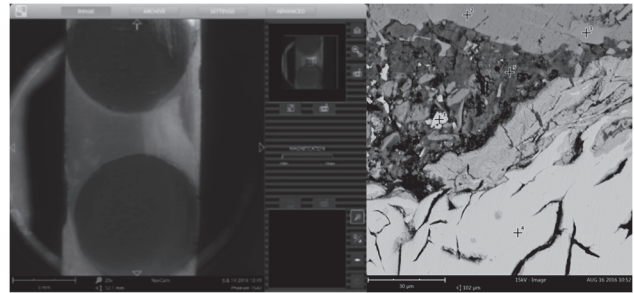


Figure 4 Photography of cylinder liner sample consisting of two materials for EDS analysis and SEM observation of the counterpart under constant normal load of  $F_N = 0.3 \text{ N}$

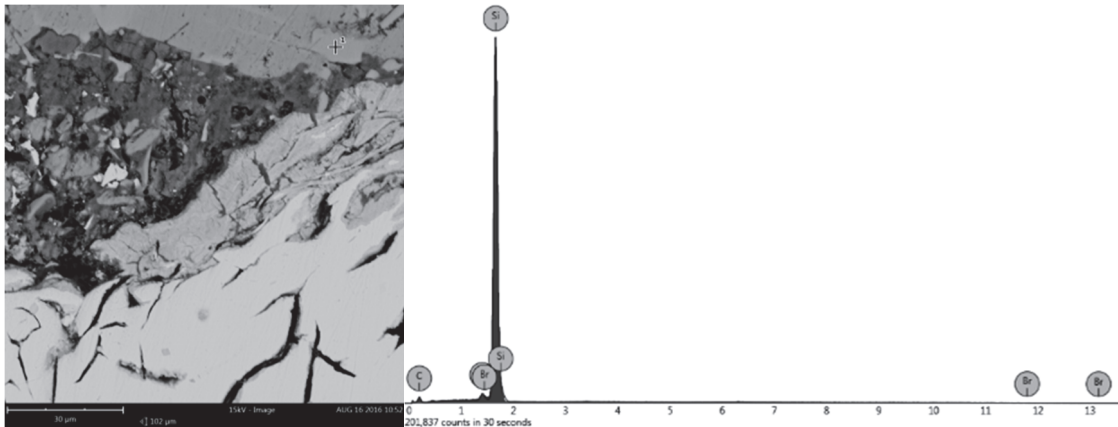


Figure 5 SEM/EDS analysis of the characteristic point 1 on the micrograph of tested material sample, Fig.4 Atomic percentage: C = 49.8%; Si = 49.4% and Br = 0.8%

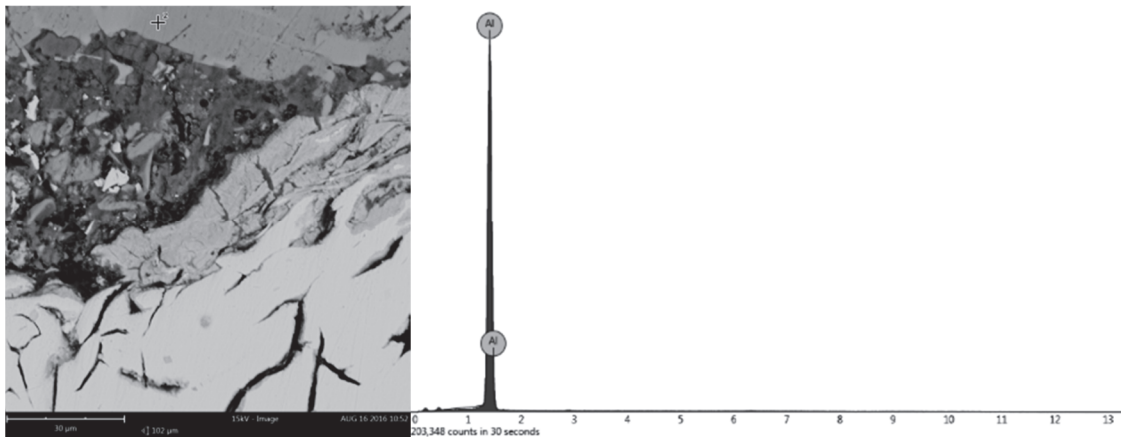


Figure 6 SEM/EDS analysis of the characteristic point 2 on the micrograph of tested material sample, Fig. 4 Atomic percentage: Al = 100%

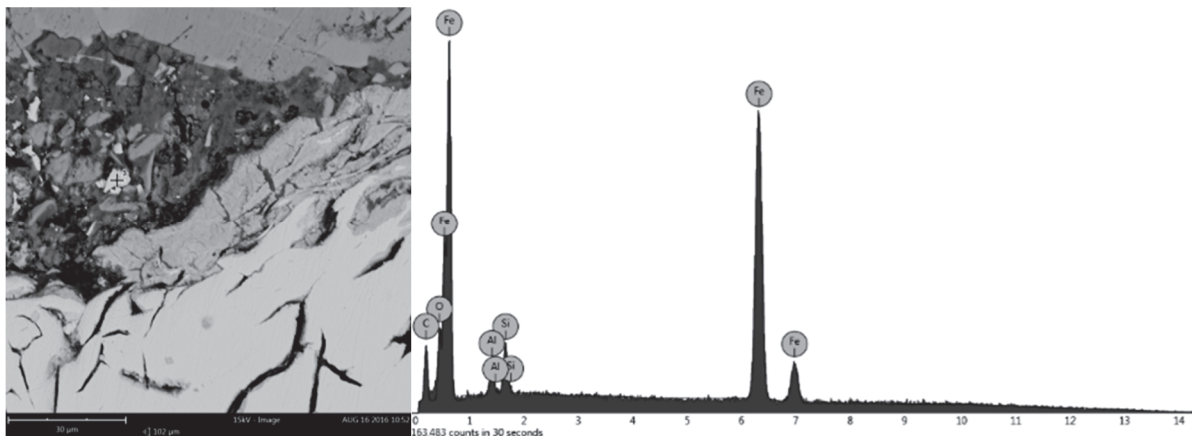
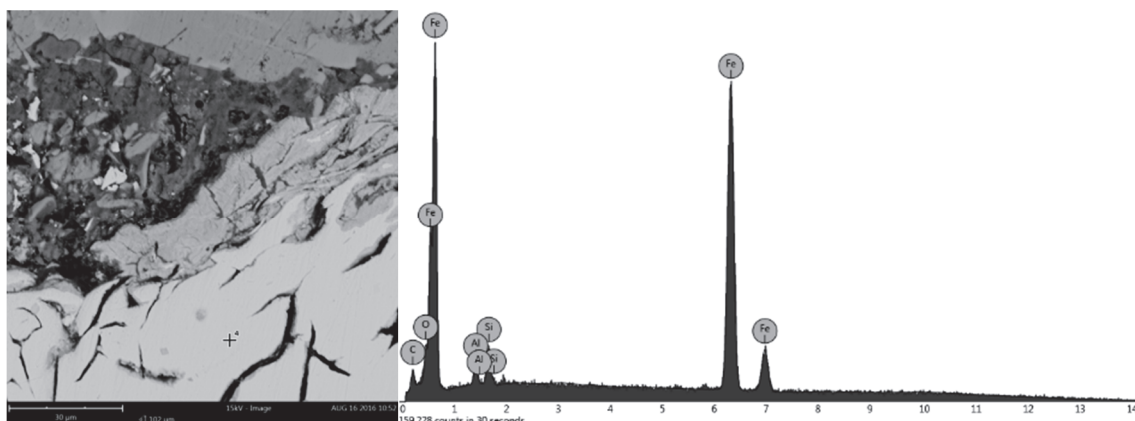
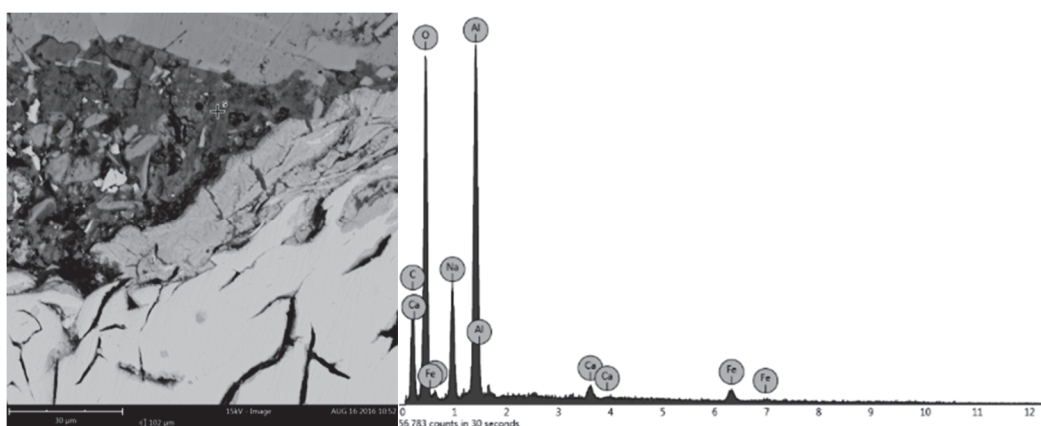


Figure 7 SEM/EDS analysis of the characteristic point 3 on the micrograph of tested material sample, Fig. 4 Atomic percentage: C = 41.6%; Fe = 38.7%; O = 14.8%; Si = 2.7% and Al = 2.3%



**Figure 8** SEM/EDS analysis of the characteristic point 4 on the micrograph of tested material sample, Fig. 4 Atomic percentage: Fe = 64.5%; C = 19%; O = 10.3%; Si = 3.5% and Al = 2.6%



**Figure 9** SEM/EDS analysis of the characteristic point 5 on the micrograph of tested material sample, Fig. 4 Atomic percentage: O = 45.7%; C = 39.8%; Al = 8.6%; Na = 4.9%; Fe = 0.7% and Ca = 0.3%

According to EDS analysis of the characteristic point 1 on the micrograph of tested material sample, lighter grey zone represents eutectic silicone (consisting element in aluminum alloy) in lamellar form with graphite inclusions, Fig. 5. Dark grey zone in the point 2 represents pure aluminum, Fig. 6. White lamella in the point 3 represents cast-iron particles in aluminum alloy with graphite, because of performed grinding process, Fig. 7.

White phase in the point 4 in Fig. 8 represents pure iron oxide inside reinforcement, although graphite is present, too. This phenomenon is present in all investigated material samples of reinforcement. Black phase represents graphite, Fig. 9. The higher presence of graphite at point 5 is caused by a performed grinding and cleaning process on the tested material surface.

### 3.2 Penetration Depth and Friction Coefficients of the Tested Aluminum Alloy as Base Material of the Compressor Cylinder

Tests which were performed at constant normal load, first at lower and after that under higher sliding speed, are reported in Fig. 10 for aluminum alloy (Al-Si) as base material of the compressor cylinder and in Fig. 11 for reinforcement. The acquired signals of friction coefficient and penetration depth (PD) (on ordinates) are reported as the function of time and lap number (contact cycles) and sliding distance.

Under material testing, a lower load was applied on the counterpart of tribometer (sphere), or low constant normal force of 0.3 N. The overall distance of reciprocating motion

was set to 1 m, at two sliding speed values of 0.003 and 0.015 m/s.

Due to the reciprocating motion of the cantilever of the tribometer, Fig. 3, the direction of friction force changed during testing. In this way, the conditions in the cylinder of the reciprocating compressor are partly simulated. A similar movement is performed by the piston in the cylinder of an internal combustion engine. During low load and 0.003 m/s constant minimal test sliding speed of the tribometer sphere (ball), friction coefficient and penetration depth of cylinder material have relatively constant and steady state values. The recorded value (mean value) of the friction coefficient is 0.110, Fig. 10a. At higher sliding speed of 0.015 m/s, the friction coefficient first increases intensively with sliding distance under running period and after about 300 mm achieves steady state mean value, Fig. 10b. If both cases are compared, more different values of the friction coefficient (0.110 and 0.350) were reached, depending on sliding speed. The increase of sliding speed under low and constant load results in increases of maximal (0.123-0.543) and mean values of the friction coefficient (0.110-0.350). A similar friction behavior under higher load was partially reported inside other published researches [21, 22].

In case of higher sliding speed 0.015 m/s penetration depth value is higher and there exists no steady state value, due to the intensive material transfer to the harder tribometer ball. The main reason is that the tested material (aluminum alloy) is softer than the material of the tribometerball.

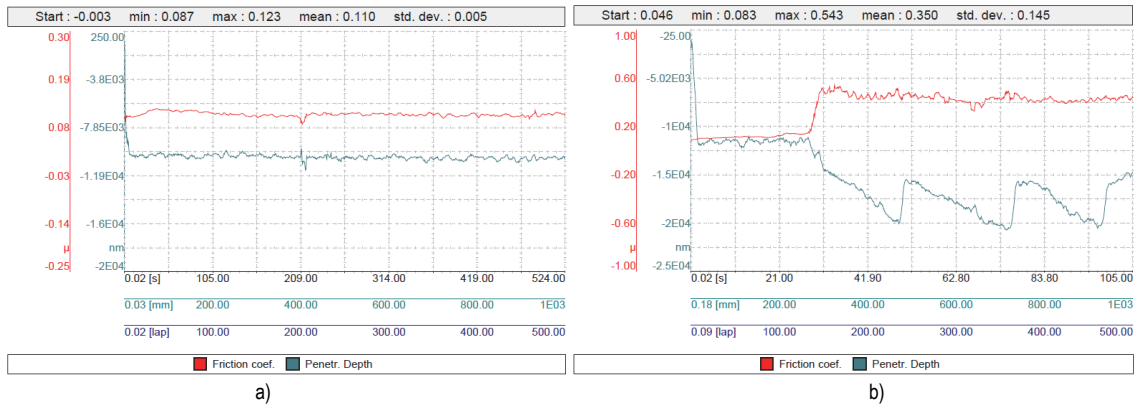


Figure 10 Dependence of friction coefficient and penetration depth changes on the sliding distance, time and cycles, for cylinder material during constant load test; a) 0.3 N and 0.003 m/s; and b) 0.3 N and 0.015 m/s

### 3.3 Penetration Depth and Friction Coefficients of Ferrous Based Reinforcements which are Integrated Inside the Cylinder Wall

Friction coefficient (0.285) of material for cylinder reinforcement, under testing with low sliding speed of 0.003 m/s, is higher, Fig. 11a. The conclusion was based on the recorded value of the friction coefficient (0.110) of the cylinder material under the same test conditions, Fig. 10a.

A similar result was achieved when testing the reinforcement material at the higher sliding speed of 0.015 m/s. In this condition friction coefficient (0.232) as well as its maximal value (0.295), Fig. 11b for reinforcement is also significantly lower, compared to result with base material (0.350) and (0.543) respectively, Fig. 10b.

Under higher sliding speed COF first increases with sliding distance rise and after about 300 mm achieves steady state mean value, Fig. 11b.

In both cases in Fig. 11, test results on reinforced samples show that the penetration depth values are almost constant. However, this is not the case with the cylinder material, especially at higher sliding speed of 0.015 m/s,

where larger oscillations in the value of penetration depth are recorded, Fig. 10.b. The fact is that no material transfer was observed during the testing of the reinforcement material made of cast-iron, Fig. 13. It can be concluded that due to the higher strength of the reinforcement material, it is not susceptible to the appearance of plastic deformations during testing.

Therefore, the reinforcement material is not subject to adhesive wear, Fig. 13, as is the case with the cylinder material, according to Fig. 12.

Fig. 13 shows the scratched surface of the reinforcement sample, with the obvious presence of parallel and equal lines, which are not observed clearly when testing the cylinder material, Fig. 12, due to the pronounced adhesion wear of the material. At the same load, this phenomenon is less pronounced at lower sliding speed.

Generally, a very intensive penetration depth value due to intensive wear rate was obtained for the base aluminum alloy due to the intensive material transfer to the harder ball, Fig. 14. Similar friction behavior under different load conditions was presented inside other similar researches [21, 22, 35].

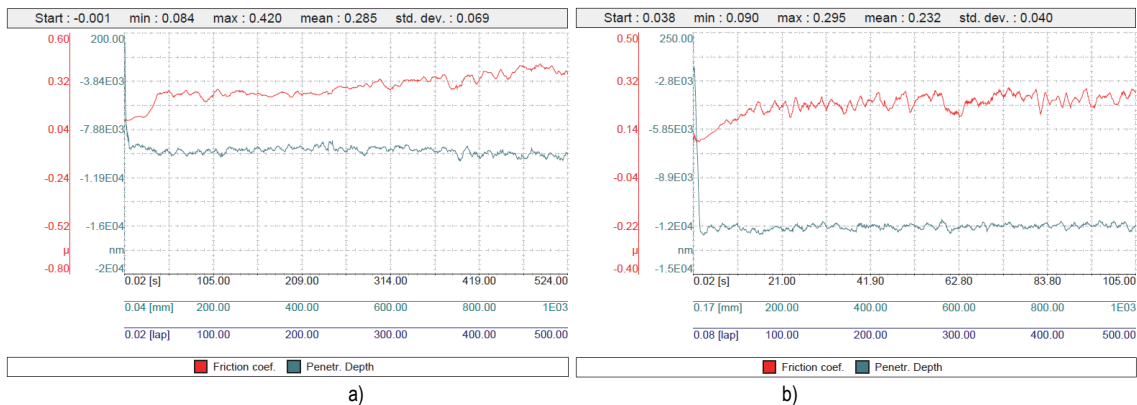


Figure 11 Dependence of friction coefficient and penetration depth changes on the sliding distance, time and cycles, for reinforcement material during constant load test; a) 0.3 N and 0.003 m/s; and b) 0.3 N and 0.015 m/s

## 4 OPTICAL MICROGRAPHS ANALYSIS OF SCRATCHED MATERIAL SURFACES AND DISCUSSION

### 4.1 Optical Microscopic Analysis of Wear Tracks for Cylinder Materials

Optical micrographs for the scratched surface of tested samples are presented in Fig. 12 and Fig. 13 for cylinder and reinforcement materials, respectively.

As explained in the previous text, due to the occurrence of material transfer and its adhesion, after tribological tests, traces of adhesive wear were recorded, Fig. 12a and 12b. This phenomenon was confirmed by a more detailed analysis of the surface of the tribometer ball after tribological tests using an optical microscope, Fig. 14. Material transfer was recorded, and this is especially noticeable at higher sliding speed, for cylinder material.

However, for reinforcement, at lower sliding speed of 0.003 m/s, the phenomenon of abrasive wear is more pronounced. In this case, the dominant phenomenon is abrasive wear, which is confirmed by parallel scratches on the surface of the tested material, Fig. 13, as well as parallel but much lighter lines on the tribometer ball, Fig. 15. This proves that the critical temperature in the contact zone of the tested materials, which is necessary for the occurrence of adhesion, has not been reached.

In this case, it is a tribological contact of two surfaces made of hard materials (tribometer ball and cast-iron reinforcement). According to the composition of the tested materials and their higher strength, smaller cracks in the form of lines of equal length can be seen on the scratching surface of reinforcement, Fig. 13. Similar traces of wear were recorded on the surface of the tribometer ball, but lighter due to minor scratches on the harder surface, Fig. 15.

In general, based on the tribological tests, less wear on the reinforcement material was confirmed, which is why it can be used for the proposed optimization of the cylinder liner construction.

The hardness of the material was determined before the start of the test using the standard procedure according to the Vickers hardness test. The average values of hardness (HV or Vickers Pyramid Number) for cylinder material and reinforcement are 90 and 318 respectively. The average values of the modulus of elasticity (Young modulus) of the tested materials are 100 GPa and 155 GPa for base cylinder material of aluminum-alloy and cast-iron inserts, respectively.

Mechanical characterization of materials and determination of mechanical characteristics of scratched surfaces were performed using the device (CSM Nano Hardness Tester or NHT), with Berkovich diamond indenter.

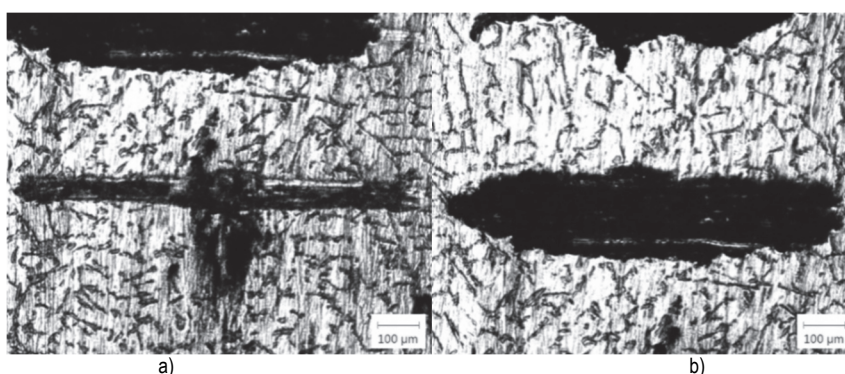


Figure 12 Optical micrograph of cylinder material surface after sliding test in constant load conditions without the presence of lubricants; a) 0.3 N and 0.003 m/s; and b) 0.3 N and 0.015 m/s

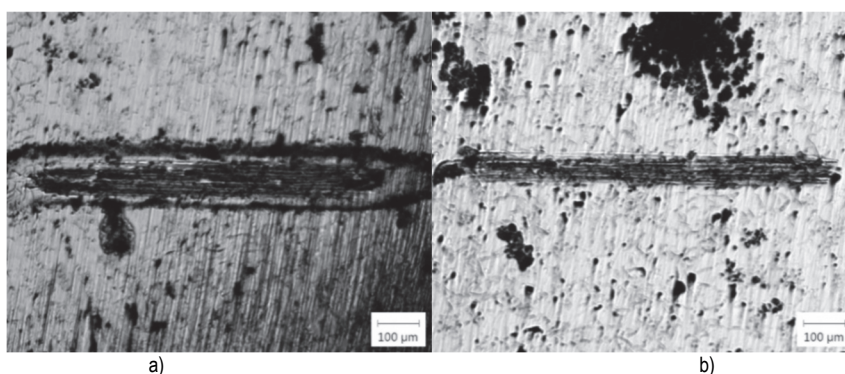


Figure 13 Optical micrograph of reinforcement material surface after sliding test in constant load conditions without the presence of lubricants; a) 0.3 N and 0.003 m/s; and b) 0.3 N and 0.015 m/s

#### 4.2 Optical Microscopic Analysis of Wear Tracks for Tribometer Sphere (Ball) Surface in Sliding Contact

In accordance with the previously mentioned conclusions, the traces of wear on the steel ball of the tribometer were additionally analyzed. The recorded traces of wear in Fig. 14 indicate a pronounced presence of material transfer on the surface of the steel ball. Accordingly, if we analyze the recorded penetration depth diagrams in Fig. 10, it can be concluded that in the case of cylinder material, the mechanism of adhesive wear is dominant.

At higher sliding speed of 0.015 m/s, an increased transfer of material to the tribometer ball was observed,

Fig. 14b. This represents clear traces of adhesive wear on the cylinder material.

During the sliding test, the transfer of material is also registered by changing the friction coefficient and penetration depth. At a certain point of time, due to the transfer of material to the tribometer ball, the sliding process occurs between the same materials. In this case, there exists sliding between Al-Si alloy as the base cylinder material and the transferred layer of the same material on the tribometer ball.

The accumulation of material on the contact surface of the tribometer ball can also be monitored by changing the penetration depth value.

If we analyze the recorded curves of changes in the penetration depth during sliding, it can be seen that the

sensor registers a sudden change in the position of the ball along the  $z$  axis of the tribometer, Fig. 3, although there is no penetration of the ball into the test material.

This is the consequence of a transferred layer of material on the ball's surface and its degradation at the

critical point. After that, it cannot transmit or overcome tangential forces. With the material transfer progress, contact area increases resulting in increased wear track width (Figs. 10, 12 and 14).

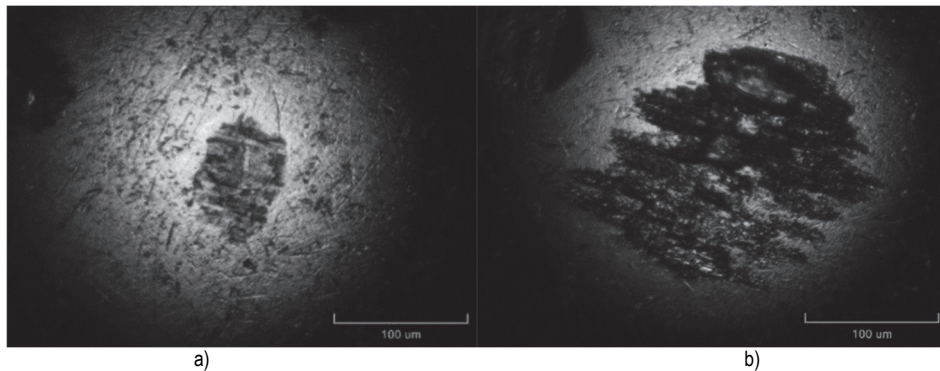


Figure 14 Optical micrographs of tribometer ball profile after sliding tests versus cylinder material (Al-Si alloy) in constant load conditions; a) 0.3 N and 0.003 m/s; and b) 0.3 N and 0.015 m/s

Material transfer was not observed in the case of cylinder reinforcement material testing. Therefore, no traces of adhesive wear can be seen on the surface of the ball, Fig. 15. A similar conclusion can be drawn from the photographs of the tested material, in Fig. 13. Therefore, the penetration depth curve is almost linear, as shown in Fig. 11. At the beginning of the testing of the cylinder reinforcement material, the friction coefficient increases until real contact is made. According to the geometry of the tribometer, at the beginning of the test, contact was made

at five points, Fig. 11. Similar results can be observed in the literature [35, 36].

This is in line with the fact that abrasive wear is dominant in the case of cylinder reinforcement materials.

After the initial time, the third layer of material is removed from the contact surface, so that the friction coefficient at a higher sliding speed is lower compared to the reference value for the cylinder material. This is especially true of maximum values Fig. 11, and 10.

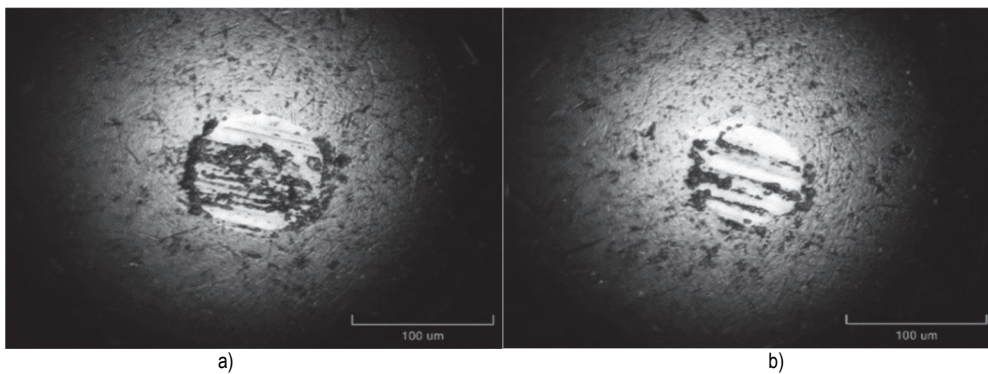


Figure 15 Optical micrographs of tribometer ball profile after sliding tests versus reinforcement material (cast-iron) in constant load conditions; a) 0.3 N and 0.003 m/s; and b) 0.3 N and 0.015 m/s

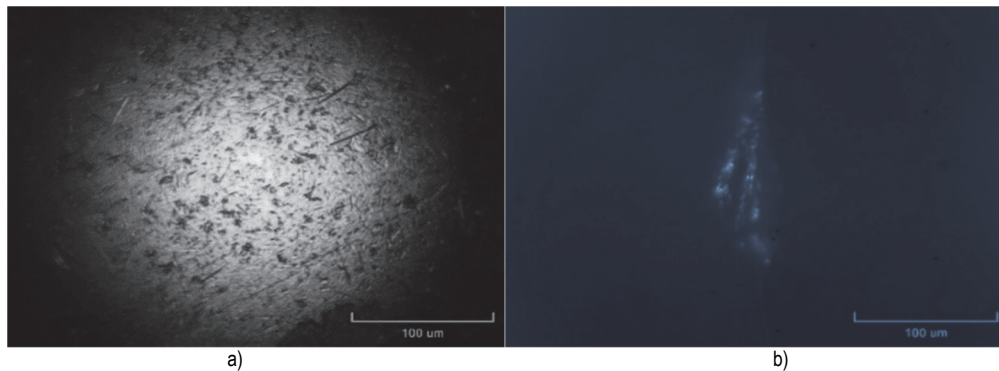


Figure 16 Optical micrographs of the tribometer ball profile; a) before sliding test (front view); and b) after sliding test (side view)

Continuing the previous analysis, Fig. 16.a and 16.b show the side profile of the tribometer ball before and after tribological tests in sliding conditions. Transfer of material to the tribometer ball can be observed [36]. Similar results

and dependencies performed by researchers under similar and different loading conditions of the tested materials can be found in the literature [22, 23].

## 5 CONCLUSIONS

Generally, on vehicles and engines, the use of new lightweight materials or eco-tribology measures (surface change for example) is important for lowering the fuel consumption, while the propulsion and mobile systems for keeping projected safety and performance.

Mechanical losses (consisting of friction and parasitic losses in auxiliary units) in internal combustion engines, can be reduced by improving tribology situation of sliding contact between two metal surfaces. On the other hand, losses can be reduced as well as lightweight of sliding parts, reducing production tolerances to improve the fit between piston-piston rings and cylinder liner, and by improving the lubrication between sliding parts.

The manuscript presents only the results of tribology research which are useful for material comparison regarding tribology characteristics (specifically friction coefficient and wear). This means that experimental results are obtained just in tribology experiments with reciprocating motion between the sphere made of steel and a plate made of tested material. For final material selection for the cylinder liner before production, we needed experimental research in real conditions.

For the purposes of the experiment, the inner or sliding surface of the Al-Si alloy compressor cylinder, (made of alloy AlSi10Mg), was modified and reinforced, by putting tribological reinforcement of cast-iron or second material (graphite or brass) as option.

The increase of sliding speed under low and constant load resulted in increases of maximal (0.123-0.543) and mean values of the friction coefficient (0.110-0.350) regarding the cylinder material Al-Si alloy. The friction coefficient mean value (0.232) for reinforcement of cast-iron material at the higher sliding speed of 0.015 m/s, is lower than the comparative value obtained by testing the cylinder material of Al-Si alloy (0.350). The maximum value of the friction coefficient (0.295) of the reinforcement is significantly lower compared to results with base material tribology tests (0.543), too.

In case of higher sliding speed of 0.015 m/s, penetration depth value for cylinder material is higher and there exists no steady state value. The main reason for this phenomenon is the intensive cylinder material transfer to the harder tribometer ball. This is due to the fact that the basic material of the cylinder is made of aluminum-silicon alloy and is softer than the material of the cylinder reinforcement on the basis of cast-iron.

Penetration depth value is almost constant during sliding test with reinforcement material. This fact does not apply to testing of cylinder material, especially in conditions of higher sliding speed during testing. The fact is that in the case of testing materials for cylinder reinforcements, no material transfer was recorded.

In the case of reinforcement material, during sliding friction, the abrasive wear mechanism dominates and no plastic deformations occur.

## Acknowledgements

The paper is a result of the research within the project TR 35041 financed by the Ministry of Science and Technological Development of the Republic of Serbia.

## 6 REFERENCES

- [1] Vehicle Technologies Office, U.S. Department of Energy. Energy Efficient Mobility Systems, from <https://www.energy.gov/eere/vehicles/energy-efficient-mobility-systems>, accessed on 2022-02-03.
- [2] Alessandro, M., Jelica, P., Biagio, C., Simone, S., & Georgios, F. (2015). Gaseous Emissions from Light-Duty Vehicles: Moving from NEDC to the New WLTP Test Procedure. *Environmental Science & Technology*, 49(14), 8315-8322. <https://doi.org/10.1021/acs.est.5b01364>
- [3] Skrúčaný, T., Kendra, M., Stopka, O., Milojević, S., Figlus, T., & Csiszár, C. (2019). Impact of the Electric Mobility Implementation on the Greenhouse Gases Production in Central European Countries. *Sustainability*, 11(18), 4948. <https://doi.org/10.3390/su11184948>
- [4] Reitz, R. D., Ogawa, H., Payri, R., Fansler, T., Kokjohn, S., Moriyoshi, Y., Agarwal, A. K. et al. (2020). IJER Editorial: The Future of the Internal Combustion Engine. *International Journal of Engine Research*, 21(1), 3-10. <https://doi.org/10.1177/1468087419877990>
- [5] Luka, L., Breda, K., Eloisa, T. J., & Fernando, C. P. (2020). Why we should invest further in the development of internal combustion engines for road applications. *Oil & Gas Science and Technology - Revue d'IFP Energies Nouvelles*, 75(56). <https://doi.org/10.2516/ogst/2020051>
- [6] Sasaki, S. (2010). Environmentally friendly tribology (Eco-tribology). *Journal of Mechanical Science and Technology*, 24, 67-71. <https://doi.org/10.1007/s12206-009-1154-1>
- [7] Joost, W. J. (2012). Reducing Vehicle Weight and Improving U.S. Energy Efficiency Using Integrated Computational Materials Engineering. *JOM*, 64, 1032-1038. <https://doi.org/10.1007/s11837-012-0424-z>
- [8] Knauder, C., Allmaier, H., Sander, D. E., & Sams, T. (2019). Investigations of the Friction Losses of Different Engine Concepts. Part 2: Sub-Assembly Resolved Friction Loss Comparison of Three Engines. *Lubricants*, 7, 105. <https://doi.org/10.3390/lubricants7120105>
- [9] Staffan, J., Per, H. N., Robert, O., & Bengt-Göran, R. (2017). A Novel Approach to Reduction of Frictional Losses in a Heavy-Duty Diesel Engine by Reducing the Hydrodynamic Frictional Losses. *Advances in Tribology*, 2017, Article ID 9240703. <https://doi.org/10.1155/2017/9240703>
- [10] Wong, V. W. & Tung, S. C. (2016). Overview of automotive engine friction and reduction trends-Effects of surface, material, and lubricant-additive technologies. *Friction*, 4, 1-28. <https://doi.org/10.1007/s40544-016-0107-9>
- [11] Richardson, D. E. (2000). Review of Power Cylinder Friction for Diesel Engines. *Journal of Engineering for Gas Turbines and Power - ASME*, 122(4), 506-519. <https://doi.org/10.1115/1.1290592>
- [12] Guo, Z. W., Yuan, C. Q., Bai, X. Q. et al. (2018). Experimental Study on Wear Performance and Oil Film Characteristics of Surface Textured Cylinder Liner in Marine Diesel Engine. *Chinese Journal of Mechanical Engineering*, 31, 52. <https://doi.org/10.1186/s10033-018-0252-3>
- [13] Zhang, Y., Fu, H., Wang, X., Liang, H., Puoza, J. C., Ji, J., Hua, X., Xu, X., & Fu, Y. (2020). Additional Tribological Effect of Laser Surface Texturing and Diamond-Like Carbon Coating for Medium Carbon Steel at Near Room Temperature. *Coatings*, 10, 929. <https://doi.org/10.3390/coatings10100929>
- [14] Gebre, F. A. (2020). Processing Methods and Mechanical Properties of Aluminium Matrix Composites. *Advances in Materials Science and Engineering*, 2020, Article ID 3765791. <https://doi.org/10.1155/2020/3765791>
- [15] Timelli, G., Fabrizi, A., Vezzù, S., & De Mori, A. (2020). Design of Wear-Resistant Diecast AlSi9Cu3(Fe) Alloys for High-Temperature Components. *Metals*, 10, 55. <https://doi.org/10.3390/met10010055>

- [16] Friedrich, K. (2018). Polymer composites for tribological applications. *Advanced Industrial and Engineering Polymer Research*, 1(1), 3-39. <https://doi.org/10.1016/j.aiepr.2018.05.001>
- [17] Chen, W., Xia, M., & Song, W. Study on the Anti-Friction Mechanism of Nitriding Surface Texture 304 Steel. *Coatings*, 10, 554. <https://doi.org/10.3390/coatings10060554>
- [18] Chérel, J., Zaccardi, J.-M., Bouteiller, B., & Allimant, A. (2020). Experimental assessment of new insulation coatings for lean burn spark-ignited engines. *Oil & Gas Science and Technology - Revue d'IFP Energies Nouvelles*, 75(2020), 11. <https://doi.org/10.2516/ogst/2020006>
- [19] Pesic, R. & Milojevic, S. Efficiency and ecological characteristics of a VCR diesel engine. *International Journal of Automotive Technology*, 14, 675-681. <https://doi.org/10.1007/s12239-013-0073-4>
- [20] Milojević, S. & Pešić, R. (2018). Determination of Combustion Process Model Parameters in Diesel Engine with Variable Compression Ratio. *Journal of Combustion*, 2018, Article ID 5292837. <https://doi.org/10.1155/2018/5292837>
- [21] Stojanović, B. & Milojević S. (2017). Characterization, manufacturing and application of metal matrix composites. *Advances in materials science research*. 30<sup>th</sup> edn. *Nova Science Publishers*, 83-133.
- [22] Milojević, S. & Stojanović, B. (2018). Determination of tribological properties of aluminum cylinder by application of Taguchi method and ANN-based model. *Journal of the Brazilian Society of Mechanical Sciences and Engineering*, 40, 571. <https://doi.org/10.1007/s40430-018-1495-8>
- [23] Vencel, A. (2015). Tribological Behavior of Ferrous-Based APS Coatings Under Dry Sliding Conditions. *Journal of Thermal Spray Technology*, 24, 671-682. <https://doi.org/10.1007/s11666-014-0202-2>
- [24] Morawitz, U., Mehring, J., & Schramm, L. (2013). Benefits of Thermal Spray Coatings in Internal Combustion Engines, with Specific View on Friction Reduction and Thermal Management. *SAE Technical Paper*. <https://doi.org/10.4271/2013-01-0292>
- [25] Kano, M. (2015). Overview of DLC-Coated Engine Components. *Coating Technology for Vehicle Applications*. Springer. [https://doi.org/10.1007/978-3-319-14771-0\\_3](https://doi.org/10.1007/978-3-319-14771-0_3)
- [26] Pešić, R., Veinović, S., & Pavlović, R. (2004). Application of aluminum alloys in production of engines and compressors. *Mobility & Vehicle Mechanics*, 30, 85-105.
- [27] Kalin, M., Polajnar, M., Kus, M., & Majdič, F. (2019). Green Tribology for the Sustainable Engineering of the Future. *Strojniški vestnik - Journal of Mechanical Engineering*, 65(11-12), 709-727.
- [28] Ma, S., Liu, Y., Wang, Z., Wang, Z., Huang, R., & Xu, J. (2019). The Effect of Honing Angle and Roughness Height on the Tribological Performance of CuNiCr Iron Liner. *Metals*, 9, 487. <https://doi.org/10.3390/met9050487>
- [29] Woś, P. & Michalski, J. (2011). Effect of Initial Cylinder Liner Honing Surface Roughness on Aircraft Piston Engine Performances. *Tribology Letters*, 41, 555-567. <https://doi.org/10.1007/s11249-010-9733-y>
- [30] MAHLE GmbH (2016) Piston design guidelines. MAHLE GmbH (eds) *Pistons and engine testing*. ATZ/MTZ-Fachbuch. Springer Vieweg, Wiesbaden. [https://doi.org/10.1007/978-3-658-09941-1\\_2](https://doi.org/10.1007/978-3-658-09941-1_2)
- [31] Schneider, E., Blossfeld, D., Lechman, D., Hill, R. et al. (1993). Effect of Cylinder Bore Out-of-Roundness on Piston Ring Rotation and Engine Oil Consumption. *SAE Technical Paper*, 930796. <https://doi.org/10.4271/930796>
- [32] ACACA Protocol™, Method for determining reciprocating air compressor pump displacement and free air delivery of an air compressor package with a pump displacement of up to 600 litre/minute and test report. Retrieved from: [http://www.amei.com.au/downloads/acaca\\_protocol.pdf](http://www.amei.com.au/downloads/acaca_protocol.pdf), accessed on 2022-01-26.
- [33] Duarte, F. J., Valencia, O. G., & Piero, R. J. (2020). Effect of the Geometric Profile of Top Ring on the Tribological Characteristics of a Low-Displacement Diesel Engine. *Lubricants*, 8, 83. <https://doi.org/10.3390/lubricants8080083>
- [34] Li, G., Gu, F., Wang, T., Lu, X., Zhang, L., Zhang, C., & Ball, A. (2017). An Improved Lubrication Model between Piston Rings and Cylinder Liners with Consideration of Liner Dynamic Deformations. *Energies*, 10, 2122. <https://doi.org/10.3390/en10122122>
- [35] Milojević, S., Džunić, D., Marić, D., Skrúčaný, T., Mitrović, S., & Pešić, R. (2021). Tribological Assessment of Aluminum Cylinder Material for Piston Compressors in Trucks and Buses Brake Systems. *Tehnički vjesnik*, 28(4), 1268-1276. <https://doi.org/10.17559/TV-20200915110030>
- [36] Vijeesh, V. & Narayan P. K. (2014). Review of Microstructure Evolution in Hypereutectic Al-Si Alloys and its Effect on Wear Properties. *Transactions of the Indian Institute of Metals*, 67, 1-18. <https://doi.org/10.1007/s12666-013-0327-x>
- [37] Karthik, B. M., Gowrishankar, M. C., Sathyashankara, S., Pavan, H., Manjunath, S., Nagaraj, S. & Manoj, G. (2020). Coated and uncoated reinforcements metal matrix composites characteristics and applications. *Cogent Engineering*, 7, 1. <https://doi.org/10.1007/s12666-013-0327-x>

**Contact information:****Saša MILOJEVIĆ**, Expert Advisor

(Corresponding author)

University of Kragujevac, Faculty of Engineering,

Department for Motor Vehicles and Engines,

Sestre Janjić 6, Kragujevac 34000, Serbia

E-mail: sasa.milojevic@kg.ac.rs

**Slobodan SAVIĆ**, prof

University of Kragujevac, Faculty of Engineering,

Department for Applied Mechanics and Automatic Control,

Sestre Janjić 6, Kragujevac 34000, Serbia

E-mail: ssavic@kg.ac.rs

**Slobodan MITROVIĆ**, prof

University of Kragujevac, Faculty of Engineering,

Department for Production Engineering,

Sestre Janjić 6, Kragujevac 34000, Serbia

E-mail: boban@kg.ac.rs

**Dejan MARIĆ**, PhD

(Corresponding author)

University of Slavonki Brod, Mechanical Engineering Faculty in Slavonki Brod,

Trg Ivane Brlić Mažuranić 2, HR-35000 Slavonki Brod, Croatia

E-mail: dmaric@unisb.hr

**Božidar KRSTIĆ**, prof

University of Kragujevac, Faculty of Engineering,

Department for Motor Vehicles and Engines,

Sestre Janjić 6, Kragujevac 34000, Serbia

E-mail: bkrstic@kg.ac.rs

**Blaža STOJANOVIĆ**, prof

University of Kragujevac, Faculty of Engineering,

Department for Mechanical Constructions and Mechanization,

Sestre Janjić 6, Kragujevac 34000, Serbia

E-mail: blaza@kg.ac.rs

**Vladimir POPOVIĆ**, prof

University of Belgrade, Faculty of Mechanical Engineering,

Department for Motor Vehicles,

Kraljice Marije 16, Belgrade11120, Serbia

E-mail: vpopovic@mas.bg.ac.rs